

Synthesis and Characterization of pH Sensitive Core–Shell–Corona Micelles of Poly(styrene-*block*-2-vinylpyridine-*block*-ethylene oxide) ABC Triblock Copolymer in Aqueous Solutions

Bhavesh Bharatiya,*[1,†] Shin-Ichi Yusa,[2] Vinod Aswal,[3] Ludmila Abezgauz,[4,5] Dganit Danino,[4,5] and Pratap Bahadur[1]

[1]Department of Chemistry, V. N. S. G. University, Surat-395007, India

[2]Department of Materials Science and Chemistry, University of Hyogo, 2167 Shosha, Himeji 671-2280

[3]SSPD, Bhabha Atomic Research Centre, Trombay, Mumbai-400085, India

[4]Department of Biotechnology and Food Engineering, Technion—Israel Institute of Technology, Haifa, Israel 32000

[5]Russell Berrie Nanotechnology Institute, Technion—Israel Institute of Technology, Haifa, Israel 32000

Received June 14, 2011; E-mail: bhaveshbharatia@yahoo.co.in

The core–shell–corona forming ABC triblock copolymer poly(styrene-*block*-2-vinylpyridine-*block*-ethylene oxide), PS–P2VP–PEO, was synthesized using reversible addition fragmentation chain transfer (RAFT) radical polymerization and characterized by NMR and GPC as PS_{13}–$P2VP_{62}$–PEO_{47}. The aggregation behavior in aqueous solution as a function of pH and temperature was studied. Turbidity measurements were used to monitor the effects associated with change in pH. The pH-sensitive P2VP block (insoluble above pH >5) and resultant protonation/deprotonation phenomenon plays decisive role in the aggregation. We found that spherical micelles of considerably low aggregation number form at pH <5. SANS and DLS characterization indicate the micelles' size and spherical shape remained virtually constant in the pH range 1 to 5. The size and shape were further confirmed by cryo-TEM.

The aggregation and phase separation of block copolymers results in a range of distinct supramolecular structures in the bulk as well as in a solvent selective for one of the blocks.[1] ABC triblock copolymers are known as precursors of quite complex self-assembled structures in the bulk.[2] Their aggregation includes the formation of "three-layer" micelles in water[3] and asymmetric micelles in organic solvents.[4]

The literature includes numerous reports comparing self-assembly of amphiphilic ABC triblock copolymers versus ABA triblock copolymers. Amphiphilic ABC triblock copolymers made of three different monomers undergo self-aggregation in aqueous solutions and form stable core–shell–corona micelles with different morphologies that can be tuned by the molecular weight, composition of blocks and solution conditions.[5] These copolymer nanoaggregates are superior to conventional micelles formed by low molecular weight surfactants. Linear amphiphilic ABC triblock copolymers are of special interest due to their simple chemical structure, which offers a variety of nanostructures in solution. Micelles with cores or coronas composed of two separate layers as well as micelles having a mixed corona can be formed based on the selectivity of the solvent with respect to the three blocks.[5] Multicompartment micelles are desirable for advanced applications in medicinal chemistry.[5,6]

Gohy et al.[6,7] reported that micelles of PS_{140}–$P2VP_{120}$–PEO_{795} and PS_{200}–$P2VP_{140}$–PEO_{590} triblock copolymers in aqueous solutions comprise a core–shell–corona structure and a spherical morphology, with PS making up the core, P2VP the shell, and PEO the corona, which showed pH and temperature dependency. The former behavior is due to the protonation–deprotonation process of the P2VP block; i.e., the P2VP block shows extended conformation at pH <5, while a collapsed conformation at pH >5. These conformational differences and dehydrating PEO block during temperature elevation make these core–shell–corona micelles temperature-responsive. A report shows ABC triblock copolymer nanoaggregates applied as vehicles for controlled drug release, and templates in the synthesis of metal nanoparticles where addition of homopolymer polystyrene prior to micellization was found to change the structure of PS–P2VP–PEO micelles to higher morphology, as a result of increased volume fraction of the PS block.[6]

Stimuli-induced morphological change of PS–P2VP–PEO micelle provides an opportunity for creating tailor-made nanoaggregates of distinct morphology. When the micelles are formed in the presence of an organic solvent selective for the PS block like benzene, the micellar morphology exhibit a sphere-to-rod transition due to increased volume fraction of the core-forming blocks.[8–11] Atomic force microscopy measurements confirmed that a PS rod-like core was covered by a P2VP shell and an external PEO corona.[7] Nevertheless, the rod-like micelles coexisted with spherical micelles that should be thermodynamically less stable, because of a higher stretching

† Present address: Institute of Condensed Matter and Nanosciences (IMCN), Universite' catholique de Louvain (UCL), Place Pasteur 1, 1348 Louvain-la-Neuve, Belgium

Published on the web October 29, 2011; doi:10.1246/bcsj.20110184

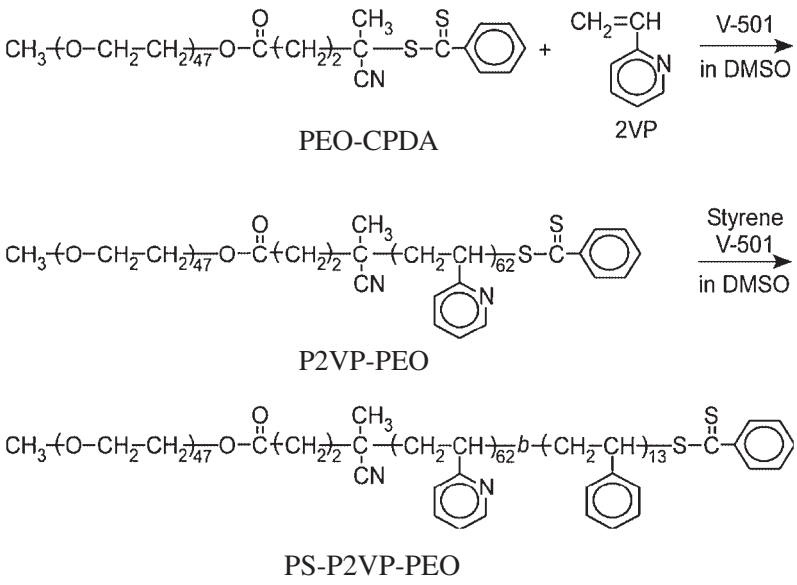

Scheme 1. Synthesis route of PS–P2VP–PEO via RAFT radical polymerization.

of the PS chains in the core. Nakashima et al.[12–14] investigated the effect of various anions on the morphology of PS–P2VP–PEO micelles by light scattering, microscopy, and fluorescence spectroscopy. As shown by Gohy et al.,[7] the P2VP block has an extended conformation at pH <5 due to the repulsion between the protonated P2VP chains. When the positive charge of the P2VP chain is diminished by some anion, the P2VP block attains shrunk conformation, and hence relatively decreased micelle size.

In this paper we report on the synthesis of poly(styrene-*block*-2-vinylpyridine-*block*-ethylene oxide) with short PS block, and its aggregation in dilute aqueous solutions as studied by turbidimetry, dynamic light scattering (DLS), small-angle neutron scattering (SANS), and cryogenic-transmission electron microscopy (cryo-TEM). The aggregation process was studied at different pH and temperature regimes. The ABC triblock micelles seem to have a more complex structure than those of AB or ABA polymeric micelles, therefore, it is interesting to investigate their physicochemical properties. The change in the structural features of the copolymer aggregates and the resultant morphologies were monitored by cryo-TEM. The pH dependent block structure and its tunable % contribution for a certain ABC copolymer can result in quite an interesting phase behavior. We synthesized ABC copolymer with sufficiently low PS contribution expecting the P2VP block to play a major role in aggregation. The literature comprising solution behavior of block copolymers in aqueous solution includes a few reports on ABC copolymers consisting ionizable block in aqueous media. Our approach is different in regards to a unique structural feature of the ABC copolymer synthesized and its characterization by scattering and microscopy techniques, which is seldom attempted earlier. Our study can add to the existing knowledge regarding the change in the structural features of ABC copolymer in aqueous media.

Experimental

4-Cyanopentanoic dithiobenzoic anhydride (CPDA) was synthesized according to the method reported by McCormick and co-workers.[15] The synthesis of poly(ethylene oxide)-based macro chain transfer agent (PEO-CPDA) was prepared according to our previous method.[16] 4,4′-Azobis(4-cyanopentanoic acid) (V-501, 98%) from Wako Pure Chemical Industries Ltd. was used as received without further purification. Styrene (99%) from Wako Pure Chemical Industries Ltd. was washed with an aqueous alkaline solution and distilled from calcium hydride under reduced pressure. 2-Vinylpyridine (2VP, 97%) from Wako Pure Chemical Industries Ltd. and dimethyl sulfoxide (DMSO) were dried over 4 Å molecular sieves and distilled under reduced pressure. The solutions for DLS and turbidimetry measurements were prepared in Milli-Q water. The copolymer solutions for SANS were prepared in D_2O obtained from heavy water division, Dhruva, BARC, Mumbai.

Synthesis of Diblock Copolymer of Poly(2-vinylpyridine) and Poly(ethylene oxide) (P2VP–PEO). 2VP (5.11 g, 48.6 mmol), V-501 (54.5 mg, 0.195 mmol), and PEO-CPDA (1.15 g, 0.486 mmol) were dissolved in DMSO (12 mL). The solution was degassed by purging with Ar gas for 30 min. The polymerization was carried out at 70 °C for 24 h. The polymerization mixture was dialyzed against pure water for one week. P2VP–PEO was recovered by freeze-drying (3.91 g, 62.0%). DP of the P2VP block is 62 as estimated by ^{1}H NMR. M_n and M_w/M_n values of P2VP–PEO are 5.97×10^3 and 1.29, respectively.

Synthesis of Triblock Copolymer of Polystyrene, Poly(2-vinylpyridine), and Poly(ethylene oxide) (PS–P2VP–PEO). The synthesis route of PS–P2VP–PEO is shown in Scheme 1. Styrene (699 mg, 6.74 mmol), V-501 (253.2 mg, 0.0899 mmol), and PEO-*b*-P2VP (1.80 g, 0.225 mmol) were dissolved in DMSO (7 mL). The solution was degassed by purging with Ar gas for 30 min. The polymerization was carried out at 70 °C for 24 h. The polymerization mixture was poured into a large excess of water to precipitate crude polymer. The precipitate was dissolved in benzene and the solution was poured into a large excess of *n*-hexane. After drying in a vacuum oven over night, PS–P2VP–PEO was obtained (1.10 g, 44.5%). DP of the PS block is 13 as estimated by ^{1}H NMR. M_n and M_w/M_n values of PS–P2VP–PEO are 6.60×10^3 and 1.51, respectively.

Proton NMR spectra were obtained with a Bruker DRX-500 spectrometer operating at 500 MHz.

GPC analysis was performed with a JASCO GPC-900 equipped with a Shodex 7.0 μm bead size GF-7M HQ column (molecular weight range of 107–102) using a 0.2 M $LiClO_4$ methanol solution as an eluent at a flow rate of 0.6 mL min^{-1} at 40 °C and a refractive index (RI) detector. The number-average molecular weight (M_n) and molecular weight distribution (M_w/M_n) for the sample polymers were calibrated with standard poly(ethylene oxide) samples.

Turbidimetry. The % transmission was recorded by Shimadzu UV-160A spectrophotometer (400 nm) at (30 ± 0.2 °C) for block copolymer solutions at different pH, using 0.1 M NaOH with vigorous stirring at regular intervals.

Dynamic Light Scattering (DLS). DLS measurements were carried out at a 90° scattering angle, using Autosizer 4800 (Malvern Instruments, U.K.) equipped with 192 channel digital correlator (7132) and coherent (Innova) Ar-ion laser at a wavelength in vacuum of 514.5 nm. The average diffusion coefficients and hence the hydrodynamic diameter was obtained by the method of cumulants.

Small-Angle Neutron Scattering (SANS). SANS experiments were performed at the Dhruva reactor, BARC, Trombay, India.[17] The solutions were held in a 0.5-cm thick quartz cell with Teflon stoppers. The diffractometer uses a polycrystalline BeO filter as a monochromator. The mean wavelength of the incident neutron beam is 5.2 Å with a wavelength resolution of approximately 15%. The angular distribution of the scattered neutron was recorded by a linear 1 m long He^3 position sensitive detector (PSD). The data were recorded in the Q range of 0.02–0.24 $Å^{-1}$. All measurements were carried out at 30 ± 0.1 °C and were corrected for the background and solvent contributions. The data were normalized to the cross-sectional unit using standard procedures. The scattering cross section per unit volume measured as a function of scattering wave vector gives micellar parameters for the monodispersed Pluronic system.[18]

In a small-angle neutron scattering experiment, one measures differential scattering cross-section per unit volume as a function of scattering vector Q, and for a monodisperse system of micelles it can be expressed as,[18]

$$\frac{d\Sigma}{d\Omega}(Q) = n(\rho_m - \rho_s)^2 V^2[\langle F(Q)^2\rangle + \langle F(Q)\rangle^2(S(Q) - 1)] + B \quad (1)$$

where "n" denotes the number density of the micelles, ρ_m and ρ_s are, respectively, the scattering length densities of the micelle and the solvent, and V is the volume of the micelle. $F(Q)$ is the single particle form factor and $S(Q)$ is the interparticle structure factor. B is a constant term that represents the incoherent scattering background, which is mainly due to hydrogen in the sample.

The block copolymer micelles can be considered as a spherical core–shell–corona particle with differing scattering length densities of core, shell, and corona. However, due to greater penetration of the solvent molecule to the corona and shell regions, the scattering length density of the corona and shell are expected to be not significantly different from that of the solvent. Thus in order to describe the core of the micelle, the form factor used was that of a monodisperse sphere as

$$F(Q) = 3[\sin(QR_c) - (QR_c)\cos(QR_c)/(QR_c)^3] \quad (2)$$

The interparticle structure factor $S(Q)$ was obtained from the analytical solution of the Ornstein–Zernike equation in the Percus–Yevick approximation employing hard sphere potential. It becomes unity in the dilute case. All the data were analyzed using nonlinear least square fitting. The core radius (R_c) was obtained by fitting the form factor $F(Q)$ and R_{hs} by fitting $S(Q)$. The aggregation number is calculated as $N_{agg} = (4/3)\pi R_c^3/v$, where v is the volume of the hydrophobic part in the micelle. The details of the analysis procedure can be found in the literature.[19–22]

Cryogenic-Transmission Electron Microscopy (cryo-TEM). Specimens for cryo-TEM were prepared in a controlled environment vitrification system (CEVS) or in the Vitrobot at a controlled temperature of 25 °C, and at saturation to avoid loss of volatiles. A drop of each solution was placed on a TEM grid covered with a perforated carbon film, blotted with a filter paper to form a thin liquid film (100–250 nm thick), and immediately plunged into liquid ethane at its freezing temperature (−183 °C) to form a vitrified specimen. The vitrified specimen was transferred to liquid nitrogen (−196 °C) for storage, then examined in the Philips CM120 or the FEI Tecnai 12 transmission electron microscopes operating at 120 kV. We used an Oxford CT3500 cryo-specimen holder that maintained the vitrified specimens below −175 °C during sample transfer and observation. Specimens were examined in the low-dose imaging mode to minimize beam exposure and electron-beam radiation damage. Images were recorded digitally[23] on a cooled Gatan MultiScan 791 CCD camera or a Gatan Ultrascan 2k × 2k cooled CCD camera, using the Digital Micrograph software.

Results and Discussion

Synthesis and Characterization. The diblock copolymer of PEO and P2VP was prepared by reversible addition fragmentation chain transfer (RAFT) radical polymerization. The polymerization of 2VP was performed in the presence of PEO macro chain transfer agent in DMSO at 70 °C (Scheme 1). GPC measurements carried out for P2VP–PEO are shown in Figure 1. The M_n and M_w/M_n values for the obtained P2VP–PEO are 5.97×10^3 and 1.29, respectively.

Preparation of a triblock copolymer of PS–P2VP–PEO using P2VP–PEO macro chain transfer agent is shown in Scheme 1. The sample solution was heated to 70 °C for 24 h under Ar atmosphere.

^{1}H NMR measurements of PS–P2VP–PEO were performed in DMSO-d_6 (Figure 2). The values of composition of PEO, P2VP, and PS were 47, 62, and 13 respectively, estimated from ^{1}H NMR spectrum. GPC measurements for PS–P2VP–PEO are also presented in Figure 1. The values of M_n and M_w/M_n are 6.60×10^3 and 1.51, respectively.

Effect of pH on the Micelles in Aqueous Solution. The copolymer contains a hydrophilic PEO block, hydrophobic PS block (low mol wt), and pH dependent hydrophilic/hydrophobic P2VP block. At pH 1, the polymer readily dissolves. Solutions at higher pH were prepared by dropwise addition of NaOH under constant stirring. However, the solution turned turbid at pH 5.5.

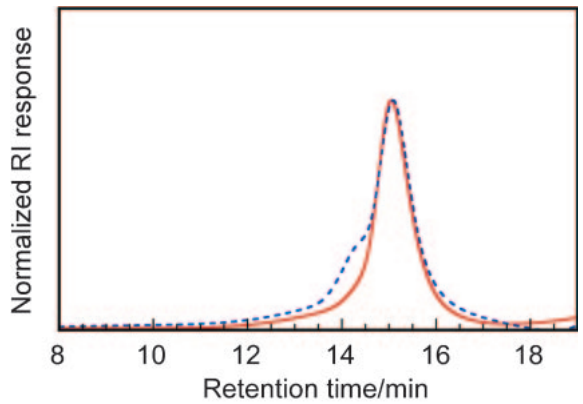

Figure 1. GPC elution profiles for P2VP–PEO (—) and PS–P2VP–PEO (----) using a 0.2 M $LiClO_4$ methanol solution as an eluent.

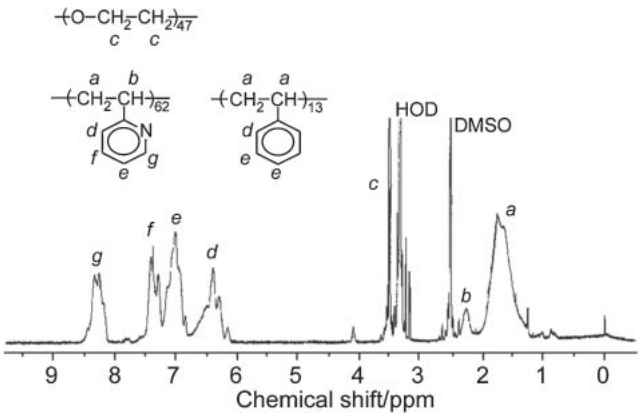

Figure 2. ^{1}H NMR spectrum for PS–P2VP–PEO in DMSO-d_6 at 100 °C.

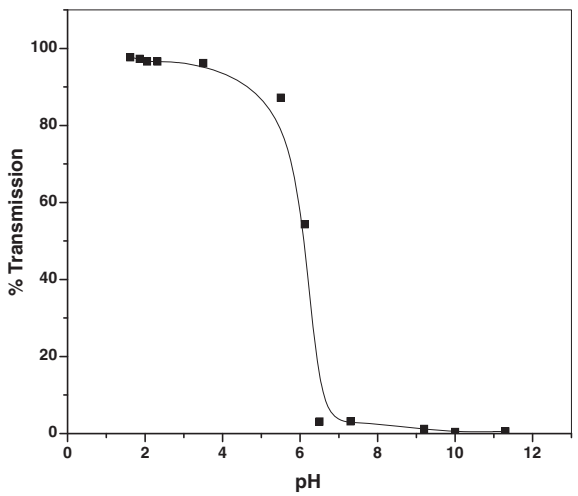

Figure 3. Turbidity measurement of 0.5 wt % PS–P2VP–PEO in water, at different pH.

Figure 3 shows the changes in % transmission of 0.5 wt % PS–P2VP–PEO as a function of pH. With increase in pH, a very slow decrease in the % transmission is observed up to pH 4. Around pH 5.5, a sudden fall in % transmission is seen. On increasing the pH further, almost zero transmittance is observed. This behavior is explained in terms of protonation–deprotonation behavior of the ionizable P2VP block. At pH 2 or less, the P2VP remains almost completely protonated and has an extended conformation.[6,24] Martin and co-workers have shown strong dependence of pH on P2VP solubility in water.[25]

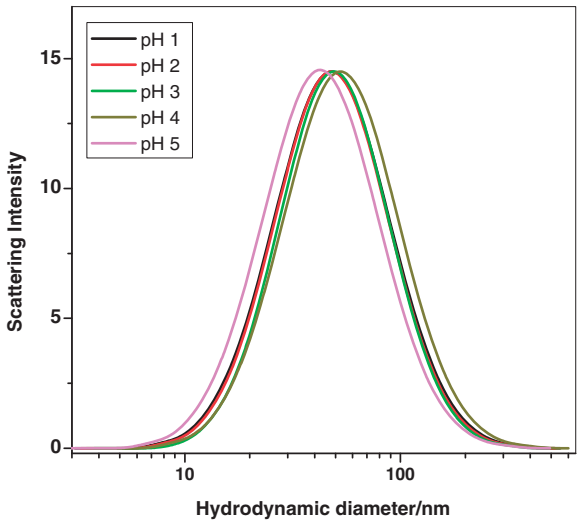

Figure 4. Scattering intensity distribution curves for 0.5 wt % PS–P2VP–PEO, at different pH, and 30 °C.

The polymer is uncharged and insoluble in water at pH >5 and gets ionized and becomes water-soluble at pH <5. However the ionization/deprotonation of P2VP is a complex process.[26] On increasing pH, deprotonation occurs, leading to the formation of dense and shrunken morphology of micelles, resulting in the observed decrease in % transmission. Above pH 5.5, P2VP becomes completely hydrophobic and collapses on the PS core. Ultimately, the PS–P2VP–PEO block copolymer becomes insoluble in water. Thus, the copolymer exhibits a pH dependent conformation of P2VP, and the shell surrounding the PS core could be heavily hydrated or collapsed. The results can be understood in light of P2VP block becoming less hydrated on increasing the pH: as pH increases, the P2VP block loses affinity for the water molecules and collapses on the PS core.

Micelle size and distribution were studied at different pH values by dynamic light scattering (DLS). The size of the micelles was around 50 nm for the whole pH range. As DLS takes into account the whole hydrodynamic volume for the calculation of micellar size, the observed value was higher than the one obtained by SANS and cryo-TEM as discussed later, though a wide distribution of scattering intensity may be due to higher polydispersity. The intensity correlation functions for 0.5 wt % PS–P2VP–PEO are shown as a function of pH in Figure 4. The distribution plots almost overlap, indicating similar size and no significant changes in the polydispersity of micelles between pH 1 to 5, which showed the values in the range of 0.3–0.35. The micellar size at pH 4, shows increase due to deprotonation of the P2VP blocks. At lower pH values, the P2VP block remains highly hydrated. The protonation of the P2VP block is decreased at pH 4, a value close to pH 5.5 when P2VP loses solubility entirely. The higher contribution of the P2VP block in polymer backbone and deprotonation favor increase in the hydrophobic interaction between the block

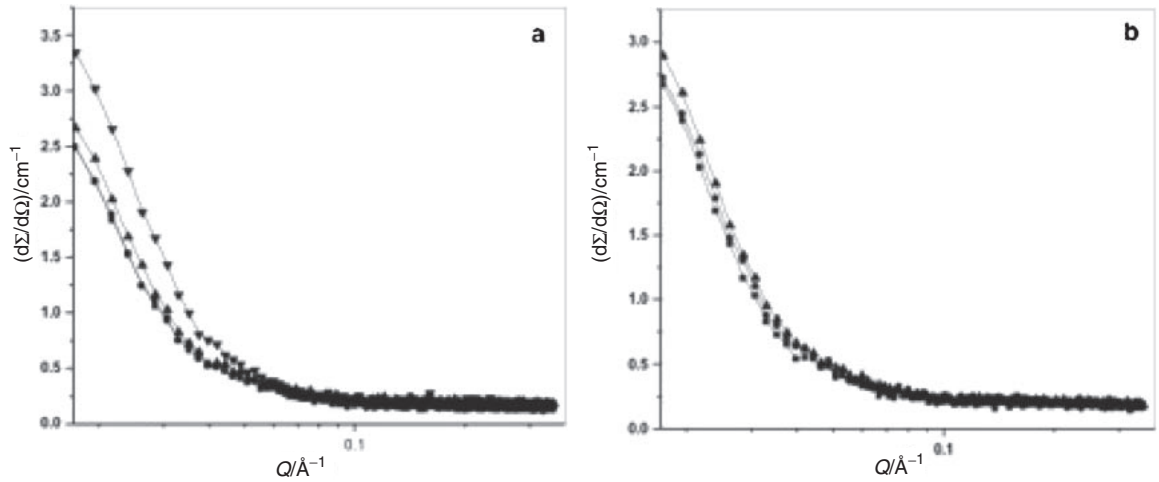

Figure 5. SANS plots for 0.5 wt % PS–P2VP–PEO in D_2O: (a) At 30 °C, different pH values equal to (■) 2, (●) 3, (▲) 4, and (▼) 5; (b) at pH 4, different temperatures (°C) equal to (■) 30, (●) 45, and (▲) 60.

copolymer molecules, which eventually allows a few more molecules to aggregate. Gohy and co-workers reported that the pH-dependent P2VP block and the contribution of all three blocks to the architecture of block copolymer play important roles in determining the aggregation behavior.[7] The small PEO block compared to P2VP and PS block being least contributor in the backbone could be the factor for constant micellar size with change in pH. Gohy et al.[6,7] investigated micellar behavior of PS_{140}–$P2VP_{120}$–PEO_{795} and PS_{200}–$P2VP_{140}$–PEO_{590}, which showed micelles below and above pH 5. Large contribution of PEO block allowed solubility of the copolymer at pH >5, when P2VP becomes totally hydrophobic. In our study, the block contribution of PEO block is even less than P2VP block and hence the copolymer phases separate after pH 5.5. During protonation of P2VP block, the PEO reside far away from PS core proximity which should increase conformational entropy. The low PS contribution compared to P2VP/PEO means that highly hydrophilic environment is dominant, which hiders the aggregation and eventually the micellar size does not show an increase. Turbidimetry measurements show a sudden fall in % transmission around pH 5. Here, the hydrodynamic size seems to remain unchanged even at pH very close to that inducing phase separation and % transmission to fall abruptly. It was also observed that the size of these micelles is independent of concentration in the range of 0.2–2% (data not shown).

The change in the micelles' morphology was further investigated by SANS. Figure 5a shows a scattering intensity vs. wave vector plot for 0.5 wt % PS–P2VP–PEO in D_2O at different pH. The core radius and other parameters were calculated from the scattering data using a SANS program written in FORTRAN. As the P2VP block remains soluble along with PEO chains, the observed micelles can be considered as a spherical core–shell particle with different scattering length densities of the core and the shell. The calculated scattering length densities for the PS, P2VP, and PEO blocks was found to be 1.2213×10^{10}, 1.6517×10^{10}, and $0.6119 \times 10^{10}\,cm^{-2}$, respectively. The form factor $F(Q)$ comprises four terms: the self-correlation of the core, the self-correlation of the chains, the cross term between core and chains, and the cross term between different chains. The structure factor $S(Q)$ of the spherical micelles in eq 1 is calculated using the Percus–Yevick approximation for the case of hard sphere potential in the Ornstein–Zernike equation.[20]

It can be seen that the scattering intensities show a very small increase upon changing the pH from 2 to 5. This minor increase in the scattering intensity may be attributed to the deprotonation upon increasing the pH. The P2VP block becomes hydrophobic to attain shrunken form. The micellar parameters were calculated considering the developed structures in spherical form. The information reveals that a few molecules of the block copolymer aggregate. The low aggregation number is attributed to polymer blocks which remain highly hydrated and do not favor aggregation. In other words, a cluster/aggregate with very low aggregation number is formed due to lack of hydrophobic environment for the measured pH range. At pH 5, the aggregation number increases to 16, which is consistent with the explanation that the increase in pH results in deprotonation of P2VP block and favorable conditions for copolymer blocks to assemble. The observed scattering intensity is quite low when compared to PEO–PPO–PEO type Pluronic block copolymers, where PPO plays a major role in the micellization and even PEO shows dehydration at elevated temperatures and in the presence of other external stimuli viz. salts, oils, hydrotropes.[5,27,28] The morphology of these developed structures was further investigated by cryo-TEM measurements, as discussed below.

Figure 5b shows a SANS plot for 0.5 wt % PS–P2VP–PEO in D_2O at different temperatures, at pH 4. The observed changes in the scattering intensity can be explained by dehydration of the PEO block with temperature elevation. PEO loses water molecules due to elevation in temperature and resultant breaking of hydrogen bondings. The scattering profile, indeed, shows temperature dependency. Though this phenomenon can be partially explained by dehydration of the water-soluble PEO block, it is a comparatively small contribution in the molecular structure that is not expected to trigger noticeable change in the micellar aggregation. The PEO and P2VP blocks play major roles at the experimental conditions (the pH and temperature range); as a result, hydrophilic environment is evident and proves to be dominant over the aggregation

Table 1. Micellar Parameters of 0.5% Copolymer Aqueous Solutions Obtained by SANS

Temp/°C	pH	R_c[a)]/Å	R_{hs}[b)]/Å	N_{agg}[c)]
30	2	10.5	69.7	2
30	3	10.6	70.0	3
30	4	10.9	70.0	3
30	5	22.3	49.6	16
45	4	12.8	62.7	4
60	4	15.2	61.3	4

a) R_c: Core radius. b) R_{hs}: Hard sphere radius. c) N_{agg}: Aggregation number.

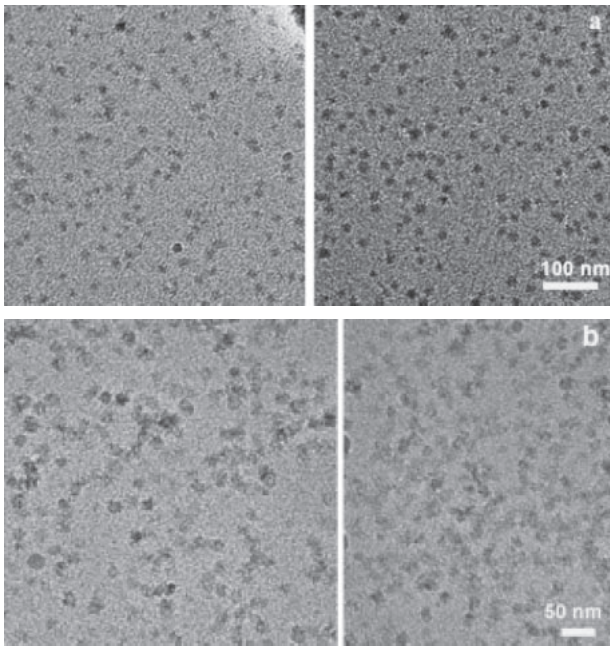

Figure 6. (a) Cryo-TEM images of 0.5 wt% PS–P2VP–PEO aqueous solution at pH 1. (b) Cryo-TEM images of 0.5 wt% PS–P2VP–PEO aqueous solution at pH 5.

phenomenon. Data analysis reveals that the temperature does not affect the aggregation to a great deal and the overall micellar size remains unaffected with increase in temperature. The aggregation parameters obtained by this analysis are shown in Table 1. The size obtained from DLS and SANS is quite different considering a highly hydrated environment, which is predominant in DLS and measures the overall hydrodynamic size of the micelle. In SANS, the observed core radius for PS core could be understood considering small contribution in the overall architecture of the copolymer.

Cryo-TEM has been a widely used technique for visualization of block copolymer micelles for the last two decades.[29–33] Cryo-TEM images of a 0.5 wt% ABC triblock copolymer solution at pH 1 displayed in Figure 6a show a homogeneous population of spherical micelles. Interestingly, only the dense core is visible, as is often the case with polymer micelles. The micelles are ≈10 nm in diameter, in good agreement with the core dimension calculated by SANS. The corona is not detected because it is highly hydrated. Figure 6b presents cryo-TEM images of the 0.5% copolymer solution at pH 5. Here again, structures with spherical geometry are seen, similar to those detected at pH 1. This is in support of the DLS and SANS results showing almost constant size of the spherical micelles over the pH range 1–5, where P2VP remains soluble due to protonation. The reason could be the highly hydrated P2VP blocks, which dominate the block copolymer structure. The resultant lack of hydrophobicity could be the factor responsible for constant micellar size over the whole experimental pH range.

Conclusion

The ABC triblock copolymer PS–P2VP–PEO was synthesized using the reversible addition fragmentation chain transfer (RAFT) method, and was characterized using NMR and GPC as PS_{13}–$P2VP_{62}$–PEO_{47}, DLS, SANS, and cryo-TEM. The pH dependent solubility of the P2VP block and a resultant protonation at pH <5.5 yields spherical polymer aggregates of small aggregation number. The size of the spherical aggregates was virtually independent of the change in pH for the soluble P2VP case, which remains insoluble over pH >5.5. We conclude that the pH dependent solubility of the P2VP block due to protonation/deprotonation plays a decisive role in the aggregation process. SANS and DLS confirmed a low aggregation number for the micelles. Cryo-TEM images show highly hydrated spherical micelles and confirm the shape uniformity over the whole pH range, which involves soluble P2VP block. The results can be helpful for deriving nanoaggregates of block copolymers in aqueous solutions, and further, they provide an opportunity to use such developed structures as templates for nanoparticle synthesis. Our next step would be to evaluate the possibility of using these developed structures toward nanotechnology routes.

PB thanks UGC-DAE CSR, Mumbai center for financial assistance (Project No. CRS-M-125). Authors gratefully acknowledge Dr. P. A. Hassan, Chemistry Division, BARC for his kind support in the DLS measurements. DD acknowledge the support of the RBNI and the Israel science Foundation No. 1137/08.

References

1 I. W. Hamley, *The Physics of Block Copolymers*, Oxford University Press, Oxford, **1998**.

2 S. I. Stupp, V. LeBonheur, K. Walker, L. S. Li, K. E. Huggins, M. Keser, A. Amstutz, *Science* **1997**, *276*, 384.

3 G.-e. Yu, A. Eisenberg, *Macromolecules* **1998**, *31*, 5546.

4 R. Erhardt, A. Böker, H. Zettl, H. Kaya, W. Pyckhout-Hintzen, G. Krausch, V. Abetz, A. H. E. Müller, *Macromolecules* **2001**, *34*, 1069.

5 J.-F. Gohy, *Adv. Polym. Sci.* **2005**, *190*, 65.

6 J.-F. Gohy, N. Willet, S. Varshney, J.-X. Zhang, R. Jérôme, *Angew. Chem., Int. Ed.* **2001**, *40*, 3214.

7 J.-F. Gohy, N. Willet, S. Varshney, J.-X. Zhang, R. Jérôme, *e-Polym.* **2002**, 35.

8 Z. Zhou, Z. Li, Y. Ren, M. A. Hillmyer, T. P. Lodge, *J. Am. Chem. Soc.* **2003**, *125*, 10182.

9 L. Lei, J.-F. Gohy, N. Willet, J.-X. Zhang, S. Varshney, R. Jérôme, *Macromolecules* **2004**, *37*, 1089.

10 L. Lei, J.-F. Gohy, N. Willet, J.-X. Zhang, S. Varshney, R. Jérôme, *Polymer* **2004**, *45*, 4375.

11 M. Štěpánek, J. Humpolícková, K. Procházka, M. Hof, Z. Tuzar, M. Špírková, T. Wolff, *Collect. Czech. Chem. Commun.* **2003**, *68*, 2120.

12 A. Khanal, Y. Li, N. Takisawa, N. Kawasaki, Y. Oishi, K. Nakashima, *Langmuir* **2004**, *20*, 4809.

13 Y. Li, A. Khanal, N. Kawasaki, Y. Oishi, K. Nakashima, *Bull. Chem. Soc. Jpn.* **2005**, *78*, 529.

14 A. Khanal, K. Nakashima, N. Kawasaki, Y. Oishi, M. Uehara, H. Nakamura, Y. Tajima, *Colloid Polym. Sci.* **2005**, *283*, 1226.

15 Y. Mitsukami, M. S. Donovan, A. B. Lowe, C. L. McCormick, *Macromolecules* **2001**, *34*, 2248.

16 S.-i. Yusa, M. Sugahara, T. Endo, Y. Morishima, *Langmuir* **2009**, *25*, 5258.

17 V. K. Aswal, P. S. Goyal, *Curr. Sci.* **2000**, *79*, 947.

18 S. H. Chen, T. L. Lin, in *Methods of Experimental Physics B*, ed. by D. L. Price, K. Skold, Academic Press, New York, **1987**, Vol. 23, p. 489.

19 J. S. Pedersen, M. C. Gerstenberg, *Macromolecules* **1996**, *29*, 1363.

20 J. K. Percus, G. J. Yevick, *Phys. Rev.* **1958**, *110*, 1.

21 J. S. Pedersen, D. Posselt, K. Mortensen, *J. Appl. Crystallogr.* **1990**, *23*, 321.

22 P. R. Bevington, *Data Reduction and Error Analysis for Physical Sciences*, McGraw-Hill, New York, **1969**.

23 D. Danino, A. Bernheim-Groswasser, Y. Talmon, *Colloids Surf., A* **2001**, *183–185*, 113.

24 L. Lei, J.-F. Gohy, N. Willet, J.-X. Zhang, S. Varshney, R. Jérôme, *Polymer* **2006**, *47*, 2723.

25 T. J. Martin, K. Procházka, P. Munk, S. E. Webber, *Macromoleculs* **1996**, *29*, 6071.

26 a) M. Puterman, J. L. Koenig, J. B. Lando, *J. Macromol. Sci., Part B: Phys.* **1979**, *16*, 89. b) M. Puterman, E. Garcia, J. B. Lando, *J. Macromol. Sci., Part B: Phys.* **1979**, *16*, 117.

27 G. Riess, G. Hurtrej, P. Bahadur, *Block Copolymers* in *Encyclopaedia of Polymer Science & Engineering*, Wiley, NY, **1985**, p. 324.

28 G. Riess, *Prog. Polym. Sci.* **2003**, *28*, 1107.

29 F. J. Esselink, E. Dormidontova, G. Hadziioannou, *Macromolecules* **1998**, *31*, 2925.

30 Y.-M. Lam, N. Grigorieff, G. Goldbeck-Wood, *Phys. Chem. Chem. Phys.* **1999**, *1*, 3331.

31 M. Goldraich, Y. Talmon, *Direct-Imaging Cryo-Transmission Electron Microscopy in the Study of Colloids and Polymer Solutions* in *Amphiphilic Block Copolymers: Self Assembly and Applications*, ed. by P. Alexandridis, B. Lindman, Elsevier, Amsterdam, **2000**.

32 M. D. Determan, J. P. Cox, S. Seifert, P. Thiyagarajan, S. K. Mallapragada, *Polymer* **2005**, *46*, 6933.

33 L. Omer, S. Ruthstein, D. Goldfarb, Y. Talmon, *J. Am. Chem. Soc.* **2009**, *131*, 12466.